

Contents list available at CBIORE journal website

## Remarkable Energy Development

Journal homepage: https://ijred.cbiore.id



Research Article

# Optimization of fuel cell switching control based on power following strategy in fuel cell hybrid electrical vehicle

Leipengyun Denga,b\*, Mohd Amran Mohd Radzia,c\*, Suhaidi Shafie, Mohd Khair Hassan, Control of the Leipengyun Denga,b\*, Control of the Leipengyu

Abstract. Fuel cell hybrid electric vehicles (FCHEVs), integrating fuel cell (FC) with batteries, have attracted significant research attention due to their emission-free operation, enhanced efficiency, and quick refuelling capabilities. Efficient energy management strategies (EMSs) are crucial in allocating energy between these sources and controlling power flow from FCs and batteries. The power following control (PFC) strategy has emerged as one of the most extensively utilized approaches in automotive applications owing to its superior real-time performance, ease of calculation, and straightforward design. This paper proposes a PFC-optimized strategy focused on improving FC durability and fuel economy by optimizing the switching control to fill the gap in frequent toggling of FC caused by traditional PFC strategy. The outcomes derived from the co-simulation conducted with AVL CRUISE and MATLAB/Simulink for developing complete FCHEV model and EMS model, respectively, indicate that under the China Lightduty Vehicle Test Cycle for Passenger Car (CLTC-P), the PFC-optimized strategy, in comparison to the traditional PFC strategy, reduces battery state of charge (SOC) fluctuations by 68.93% and decreases hydrogen consumption per 100 km by 2.71%. Meanwhile, this strategy is also proven effective in other operating conditions and reduces fuel cell switching times during operation. Therefore, the PFC-optimized strategy suggested in this study contributes to better performance in battery SOC, battery life, FC durability and fuel economy.

Keywords: FCHEV, fuel cell durability, fuel economy, powertrain system, power following optimized control



@ The author(s). Published by CBIORE. This is an open access article under the CC BY-SA license (http://creativecommons.org/licenses/by-sa/4.0/).
Received: 1st Nov 2024; Revised: 15th January 2025; Accepted: 6th February 2025; Available online: 16th February 2025

#### 1. Introduction

In contemporary times, fossil fuels remain essential in fulfilling the requirements of the transportation industry, albeit at the cost of various adverse effects including atmospheric pollution, acoustic pollution, and contributing to global warming (Du et al., 2022). Additionally, the accelerated exhaustion of subterranean oil reserves owing to fossil fuel overconsumption exacerbates concerns (Hu et al., 2022). The dual challenges of environmental degradation and energy crisis present significant hurdles to the automotive industry (Yang et al., 2021). Consequently, there is considerable scholarly and industrial interest in fuel cells (FCs), hailed as an ideal alternative energy source for various transportation applications due to their zero-emission, highly efficient operation, and adaptable power ratings (Hosseini & Butler, 2019). These transportation applications, featuring a FC either individually or in conjunction with supplementary energy storage components like batteries and/or ultracapacitors (UC), are known as fuel cell electric vehicles (FCEVs) (İnci et al., 2021). As of the end of 2022, the global stock of FCEVs in major countries reached 67,315 units, growing by 36.3% compared to the previous year. South Korea led with 29,369 units, followed by the United States with 14,979 units, and China with 12,682 units ranking third globally (Chang et al., 2024). This underscores the significant role of the FCEV industry in the

decarbonization transition of the transportation sector. Mixing FCs with energy storage systems (ESS) is crucial for reducing the size of fuel cells, minimizing power system costs, and lowering hydrogen consumption (Xu et al., 2020). In FCEV hybridization, the prevailing topology involves combining FCs with batteries (FC+B units). Efficient EMS are crucial in allocating energy between these sources and regulating power flow from FCs and energy storage systems (Shen et al., 2020; Gharibeh et al., 2020; Lin et al., 2022; Tian et al., 2024)

Various EMSs have been deployed in hybrid vehicles lately. The subsequent three EMSs are frequently employed: Optimization-based (OB) method, Learning-based (LB) method and Rule-based (RB) method (Lü et al., 2020). Optimizationbased strategies can be segmented into Global Optimization Strategy (GOS) and Real-Time Optimization Strategy (Offline and Online Optimization Strategy) (Kim et al., 2023). Bizon et al. (2018) conducted an analysis of fuel efficiency in FCHEV using Perturb & Observe strategy and Global Extremum Seeking method, comparing them with the static Feed-Forward reference algorithm. The observed differences in fuel economy underline the benefit of the GOS. In the study by (Ou et al., 2018), an online adaptive Pontryagin's Minimum Principle (PMP) EMS was introduced with the aim of decreasing hydrogen consumption. To enhance the global EMS, an online identification layer was incorporated to monitor efficient

<sup>&</sup>lt;sup>a</sup>Department of Electrical and Electronic Engineering, Faculty of Engineering, Universiti Putra Malaysia, 43400, Selangor, Malaysia

<sup>&</sup>lt;sup>b</sup>Chongqing Electric Power College, Jiulongpo District Electric Power Village, 400053, Chongqing, China

<sup>&</sup>lt;sup>c</sup>Advanced Lightning, Power, and Energy Research (ALPER) Centre, Universiti Putra Malaysia, 43400, Selangor, Malaysia

Corresponding author

operation of Proton Exchange Membrane Fuel Cell (PEMFC). The online identification algorithm utilized the adaptive recursive least squares method as its foundation. The outcomes demonstrated the algorithm's ability to optimize PEMFC performance and reduce hydrogen consumption. Nonetheless, the overall complexity and computational burden of the algorithm pose challenges, particularly in online calculations (Teng et al., 2020). Regarding LB-EMSs, Praveen et al. (2019) emphasized the Reinforcement Learning (RL) strategy, highlighting its advantage of autonomously learning the optimal control policy. They also demonstrated a tangible improvement in battery life through SOC variation reduction. Neural Network Learning (NNL) was devised to emulate the fundamental operations of neurons in the brain. Utilizing driving state recognition technology, Song et al. (2018) introduced a multimode EMS for an FC extended-range EV. Different driving conditions were identified through a learning vector quantization (LVQ) neural network. Subsequently, a thermostat strategy was refined employing a genetic algorithm (GA) to efficiently allocate energy within the FCEV power system across various driving scenarios. Learning-based methods, such as the one mentioned, do not necessitate precise model knowledge, yet the process of acquiring accurate information can be challenging and requires a substantial investment of time. With regard to Rule-based strategy, it can be subdivided into fuzzy rules and deterministic rules (Peng et al., 2021). A combination of Fuzzy Logic Control (FLC) strategy and the traditional power following strategy (PFS) was adopted by Li et al. (2020) to distribute energy, and it is simulated under Highway Fuel Economy Test (HWFET) and Urban Dynamometer Driving Schedule (UDDS) through MATLAB and ADVISOR. This strategy results in better consumption of hydrogen compared with power following control consumption. Luca et al. (2022) proposed a novel approach, the Mutative Fuzzy Logic Controller (MFLC), to improve the longevity of FCs by adjusting the output membership function according to the state-of-degradation (SOD) of the FC system. MFLC was optimized using Simulink Design Optimization through a combination of a gradient descent technique and a sequential quadratic programming method. The study explores the effects of EMSs on FC degradation, indicating that the MFLC could potentially extend the FC lifetime by up to 32.8%. Zhang and Li (2019) introduced a game theory-based strategy for power flow distribution, coupled with FLC under the UDDS driving cycle. This approach has demonstrated significant benefits in reducing fuel consumption and minimizing battery degradation, thus offering substantial advantages. The PFC strategy, as one of the deterministic rule-based approaches, represents an upgraded variant of the conventional thermostat strategy (Zhang et al., 2019). It primarily regulates the FC output power in accordance

to the battery SOC and the overall power demand of the vehicle (Jung *et al.*, 2024). Furthermore, it does not require anticipation of all driving scenario and the rule formulation relies on the expertise and practical experience possessed by engineers and technicians, enabling quick responses to changing conditions without heavy computational resources.

Hence, the power following strategy, recognized for its uncomplicated design, direct execution, and exceptional real-time efficacy, is identified as a prevalent control tactic in the automotive sector (Zou *et al.*, 2023). However, this strategy also has some shortcomings. As the central goal of this approach is to sustain the SOC of the battery at a desired level, deviations below or above this target prompt corresponding adjustments in the FC output power (Geng *et al.*, 2019). This can lead to frequent FC switching, hindering its long-term viability (Zhang *et al.*, 2021).

Therefore, for enhancing the economic efficiency of the power output from the hybrid system and improving the FC durability, this study proposes a PFC-optimized strategy incorporating braking energy recovery and fuel cell power control. The whole FCHEV model in this paper is constructed within the AVL CRUISE platform and integrated with MATLAB/Simulink to incorporate the energy management algorithms. Additionally, the selection of the powertrain of the FCHEV, parametric modelling and simulation evaluation of the power system, and EMS modelling methods are primarily introduced. Furthermore, the simulation results and analysis are discussed, with the incorporation of CLTC-P driving cycle into the CRUISE platform. To comprehensively assess the proposed EMS, three driving conditions are chosen for evaluating and analyzing the FCHEV performance. Finally, the primary findings are delineated.

## 2. Methods

## 2.1 FCHEV configuration and calculations

FCHEV setup typically encompasses drive configuration and vehicle specifications. The FCHEV configuration is illustrated in Figure 1.

Such a system mainly includes mechanical and electrical sections. The mechanical drive section is the Permanent Magnet Synchronous Motor (PMSM) linked to the final drive, and then linked to the two rear wheels via a differential. The electrical part of the Li-ion battery is directly linked to the Direct Current (DC) bus, while the PEMFC interfaced with the DC bus via a unidirectional DC/DC converter. The PEMFC output voltage is decoupled from the DC bus, with the DC/DC converter managing the PEMFC power output by regulating the current.

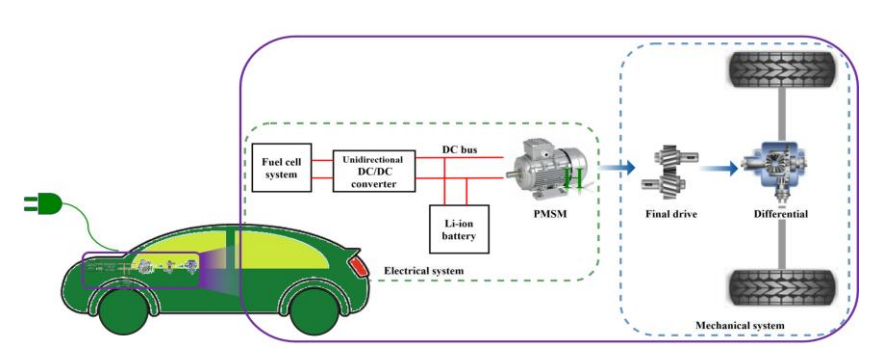


Fig. 1 FCHEV configuration

**Table 1** FCHEV Parameters

Component	Parameter	Value	
	Drive system	Rear-wheel drive	
	Curb weight (kg)	1900	
	Gross weight (kg)	2275	
	Frontal area (m²)	2.3976	
Malaiala	Wheel radius (m)	0.338	
Vehicle	Drag coefficient	0.26	
	Final drive ratio	8.5	
	Transmission efficiency	0.95	
	Rolling resistance coefficient	0.01	
	Correction coefficient of	1.05	
	rotating mass	1.00	
Motor	Туре	PMSM	
	Maximum power (kW)	160	
	Maximum speed (rpm)	12000	
	Maximum torque (Nm)	320	
FC stack	Type	PEM	
	Maximum power (kW)	80	
Battery	Туре	Lithium-ion	
	Number	120	
	Capacity (Ah)	19.5	
	Rated voltage (V)	3.75	
DC/DC converter	Efficiency	0.95	

The FCHEV parameters utilized in this research are detailed in Table 1.

Table 2 depicts the power performance index, meeting the demands of the GB/T 39132-2020 fuel cell electric vehicle engineering approval evaluation program and the GB/T 19752-2005 hybrid electric vehicles power performance test method (Duan *et al.*, 2021). The parameter matching and modeling of powertrain components are performed as follows.

## 2.1.1 Electric machine model

The design of a properly sized power unit begins with the calculation of the maximum power of the driving motor (Ahmadi *et al.*, 2018). Eq. (1) constrains this power based on the vehicle gradeability, acceleration, and maximum speed, as well as other parameters specific to the vehicle characteristics.

$$P_{m} = \frac{V}{n_{r}} \left( C_{r} \, mg cos(\theta) + 0.5 \rho C_{D} A V^{2} + mg sin(\theta) + m \delta \frac{dV}{dt} \right)$$
 (1)

where  $\eta_t$  is transmission efficiency,  $C_r$  is rolling resistance coefficient,  $C_D$  is air drag coefficient,  $\rho$  is air density, A is frontal area,  $\theta$  is slope,  $\delta$  is mass coefficient of rotary elements, V is the speed, and dV/dt is the acceleration.

Based on the driving power balance equation presented in Eq. (2), the three power values are calculated separately, with the highest value indicating the motor maximum driving power.

**Table 2**Design indicators of performance

Value Performance index Maximum speed (km/h) ≥170 0-50 km/h acceleration (s) ≤5 0-100 km/h acceleration (s) ≤10 Maximum grade (%) ≥30 Maximum grade @30km/h (%) ≥12 Maximum grade @60km/h (%) ≥4 ≥65 Cruising range @60km/h (km)

$$P_{max} = max(P_{max1}, P_{max2}, P_{max3})$$
 (2)

where  $P_{max1}$  based on maximum speed  $V_{max}$  and  $P_{max2}$  based on gradeability can be calculated as

$$P_{max1} = \frac{V_{max}}{3600\eta_t} \left( mgC_r + \frac{C_D A V_{max}^2}{21.15} \right)$$
 (3)

$$P_{max2} = \frac{V_c}{3600\eta_t} \left( mgC_r \cos\theta_{max} + mg\sin\theta_{max} + \frac{C_D A V_c^2}{21.15} \right)$$
(4)

in which  $V_C$  is climbing speed,  $\theta_{max}$  is the maximum climbing slope corresponding to the maximum grade  $i_{max}$ , and  $\theta_{max} = \arctan i_{max}$ . The maximum power  $P_{max3}$  based on acceleration performance can be described as

$$P_{max3} = \frac{V_a}{3600\eta_t} \left( mgC_r + \frac{C_D A V_a^2}{21.15} + m\delta \frac{dV}{dt} \right)$$
 (5)

where  $\delta$  is the correction coefficient of rotating mass, and  $V_a$  is the vehicle speed.

According to Equations (1)-(5), the peak power is calculated to be 140 kW. The rated power is generally the power needed during the vehicle's operation at its maximum velocity on a straight road ( $\theta$ =0). We select a PMSM rated at 80 kW with a maximum power capacity of 160 kW, taking redundancy into account

As the direct power source acting on the wheels, the maximum torque of the motor is pivotal in determining the overall dynamic performance of the vehicle. Usually,  $T_{max}$  needs to fulfill the specifications for the highest grade as Eq. (6)

$$T_{max} \ge \frac{mgC_r cos\theta_{max} + mgsin\theta_{max} + \frac{C_DAV_c^2}{21.15}}{\eta_t i_0 i_g} \times r$$
 (6)

where  $i_0$  is reduction ratio ( $i_0 = 1$ ),  $i_g$  is final drive ratio, and r is dynamic rolling radius. Given the necessity for additional torque during uphill climbs, the maximum torque is set at 320 nm, allowing for a margin of redundancy. The rated torque depends on the rated power of the motor as shown in Eq. (7)

$$T_N = \frac{9550P_N}{n_N} \tag{7}$$

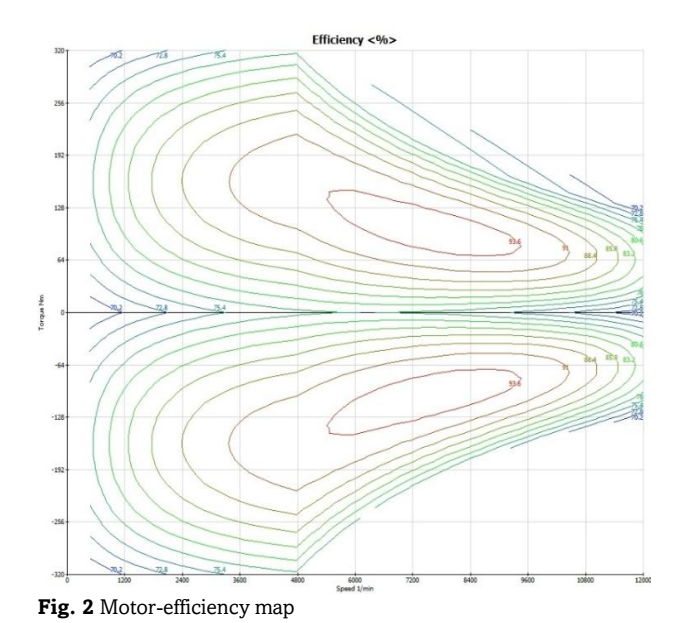
where  $P_N$  corresponds to the power required for the maximum speed, that is,  $P_{max1}$ ,  $n_N$  denotes the motor rated speed corresponding to the vehicle cruising speed and can be calculated as

$$n = \frac{v_i l_0 l_g}{0.377r} \tag{8}$$

where n is motor speed, and  $v_i$  is vehicle speed. The cruising speed in this research is 60 km/h, and the gearbox is omitted due to the lightweight consideration and the motor's ability to adjust the speed. (D. Li *et al.*, 2020). The maximum speed calculation yielded 11,175 r/min, leading to the selection of 12,000 r/min as the motor's maximum speed. Figure 2 depicts the efficiency map diagram.

## 2.1.2 PEMFC model

The FC operates as a highly intricate system comprising both a PEMFC stack and a compressor. The EMS researched in this study primarily focuses on the output attributes of the PEMFC.



The output voltage produced by the FC stack is described by (Kulikovsky, 2013)

$$U_{\text{stack}} = n_{cell}(U_{OC} - \eta_0 - j_0 R) \tag{9}$$

in which  $n_{cell}$  is the number of cells in the stack, and  $\eta_0$ ,  $U_{OC}$  and,  $j_0R$  are the cathode voltage loss, ideal open circuit voltage, and ohmic voltage loss, respectively. The power of the FC stack is characterized as

$$P_{\text{stack}} = U_{\text{stack}} \left( I_{\text{cell}} + \frac{P_{\text{com}}}{U_{\text{stack}}} \right)$$
 (10)

where  $P_{\rm com}$  is the compressor consumption, which is simulated by the "Terminal" module shown in Figure 4 (b) in the system. It changes in response to variations in the FC output power. In this study, considering the power consumption of voltage conversion during operational processes, an 80 kW FC system is necessary to generate ample power for the vehicle to achieve its top speed, eliminating the need for a secondary ESS.

## 2.1.3 Li-ion battery model

Owing to its considerable energy density and compact dimensions, the lithium-ion battery has been chosen as a supplementary power source for FCHEVs (Zhao *et al.*, 2021). The Li-ion battery serves to counterbalance the sluggish transient response of PEMFC while also harnessing energy from regenerative braking. For the purpose of model simplification, the Li-ion battery is treated as an ideal voltage source with series internal resistance (Wang *et al.*, 2023). The SOC is a crucial parameter for both the vehicle and battery EMS, and it can be calculated as Eq. (11)

$$SOC = SOC_0 - \int \frac{I_B}{Q_B} dt \tag{11}$$

where  $SOC_0$  is the SOC initial value and the  $Q_B$  denotes the rated capacity.  $I_B$  is the Li-ion battery output current, which can be calculated by

$$P_B = V_{oc}I_B - I_B^2 R_B \tag{12}$$

$$I_{B} = \frac{V_{oc} - \sqrt{V_{oc}^{2} - 4R_{B}P_{B}}}{2R_{B}} \tag{13}$$

where  $R_B$  and,  $V_{oc}$  are the internal resistance and open circuit voltage of the Li-ion battery, separately. The battery primarily functions as an additional power source for extended durations. Therefore, its maximum power should exceed the discrepancy between the PMSM maximum power during acceleration and the power of the FC system.

$$P_B = P_{max3} - \eta_{DC} P_{fc} \tag{14}$$

where  $\eta_{DC}$  is the efficiency of the DC/DC converter. The maximum power of the battery is set at around 85 kW to account for redundancy. Upon calculation, the Li-ion battery (3.75 V/19.5 Ah) was chosen as the supplementary power unit for the FCHEV. The Eq. (15) facilitates the calculation of the required number of battery cell-rows to achieve a specific capacity.

$$N_B \ge \frac{W_{65}}{W_R} \tag{15}$$

where  $W_B$  is the battery energy,  $W_{65}$  indicates the energy demand for a vehicle to traverse 65 km while maintaining a constant velocity of 60 km/h. Both can be obtained by Eq. (16-17)

$$W_B = \frac{U_B C_B \eta_{DOD}}{1000} \tag{16}$$

$$W_{65} = P_{60} \frac{d}{60} = \frac{V_{60}}{3600\eta_t} \left( mgC_r + \frac{C_D A V_{60}^2}{21.15} \right) \frac{d}{60}$$
 (17)

where  $U_{\rm B}$ ,  $C_{\rm B}$ ,  $\eta_{\rm DOD}$  and,  $P_{\rm 60}$  are battery voltage, capacity, 80% discharge depth and the power during cruising at 60 km/h respectively. The motor in this paper operates at a rated voltage of 450 V. Therefore, the battery configuration necessitates 120 cells in series and 1 in parallel.

## 2.2 Parametric modelling of FCHEV power system

Currently, vehicle simulation is frequently conducted using software such as AVL CRUISE, CARSIM, and ADVISOR (W. Li et al., 2024). AVL Cruise is engineered by AVL Company to simulate automotive operation. It utilizes a modular modeling approach, offering user-friendly operation and fast simulation speed (Y. Li et al., 2019). Once components are correctly connected, models can be validated, and simulation calculations can be performed based on designated tasks. Furthermore, this software supports connectivity with Fortran, C-Function, and MATLAB/Simulink software, providing interfaces embedding complex control algorithms. This co-simulation technology is valuable for the development and validation of vehicle control strategies, as well as the optimization of entire vehicles and powertrains. Therefore, AVL CRUISE software was selected as the primary simulation tool for this study and opts for the MATLAB DLL approach for co-simulation considering configuration complexity and simulation time. Figure 3 below outlines the modeling steps in detail.

The task calculation depicted in Figure 3 encompasses both single-task and multi-task scenarios. The matrix calculation is categorized as a multi-task calculation, which assigns a single attribute value in a certain area, such as transmission ratio and drag coefficient, enabling the comparison of multiple combination configurations. Ultimately, the selection of the most optimal matching parameters, as shown in Table 1,

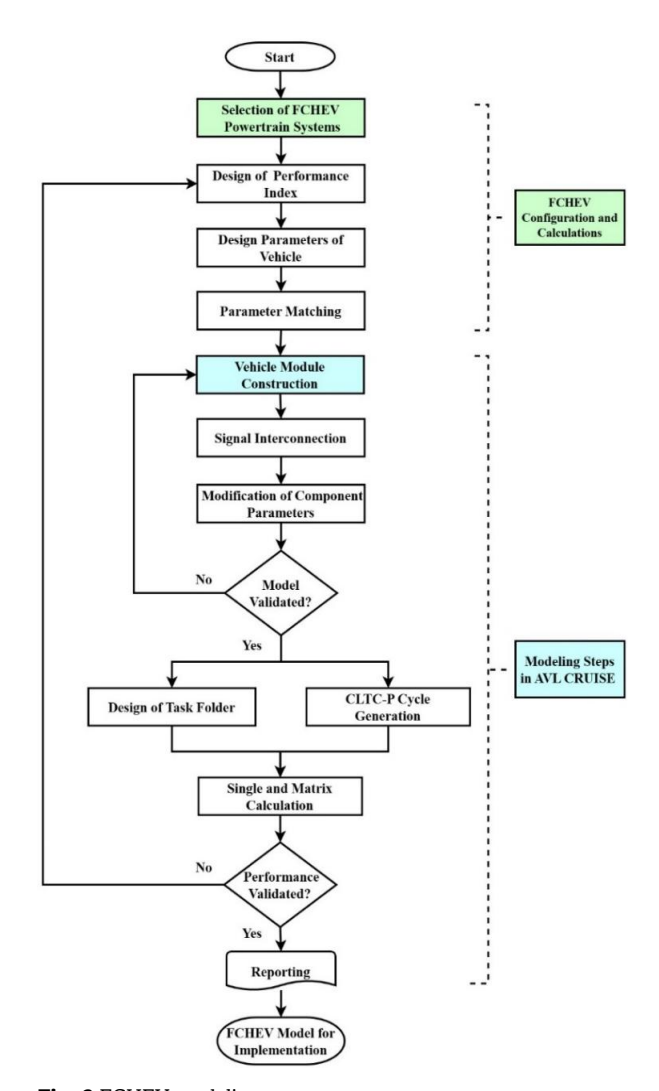


Fig. 3 FCHEV modeling steps

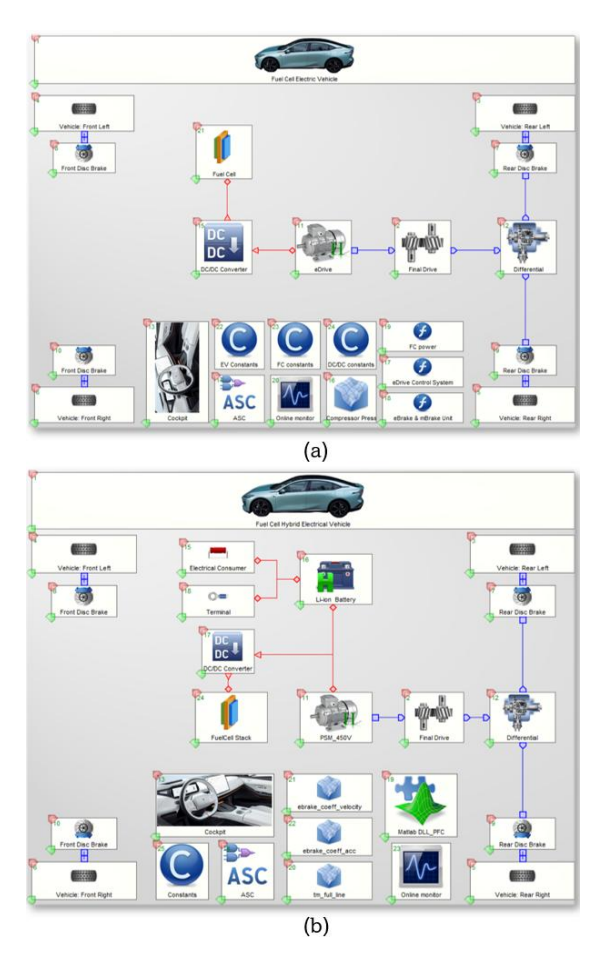
is contingent upon the diverse outcomes derived from simulation calculations.

The vehicle model exclusively powered by a fuel cell is depicted in Figure 4 (a), focusing on the singular consideration of output power control without the intricacies of coordinating power outputs from various energy sources. The core components encompass the "FCHEV" comprehensive vehicle parameter information module, "Fuel Cell Stack" module, "eDrive" PSM module, "DC/DC converter" module, "Cockpit" driver cabin module, and the transmission device module. Notably, the control strategies for the four "Disc Brake" modules and the management of braking energy recovery and distribution are configured within the "eBrake & mBrake Unit."

Figure 4 (b) illustrates the complete vehicle model, which is powered through the combined use of the battery and the FC. This contrasts with the model depicted in Figure 4 (a), significant additions include the "Li-ion Battery" module, "Electrical consumer" module, "Terminal" module, and their associated control strategies.

## 2.3 Simulation analysis of FCHEV power system

After calibrating the model, the vehicle was set to operate under the constant run task for different velocity, employing the control strategy depicted in Figure 4 (a). Brake energy recovery,



 ${\bf Fig.~4}$  Simulation model of vehicle: (a) powered by FC and (b) powered by FC+B

regenerative braking, and mechanical braking implemented using C-Function. The simulation findings suggest that as the vehicle maintains a constant speed, the energy consumption of the battery, PMSM, and electrical consumer of the vehicle converges toward a stable value (Hu et al., 2021). Figure 5 delineates the vehicle's power requirements while maintaining constant speeds at different velocities. It is obvious that the power consumption of electrical equipment is approximately 0.3 kW. It indicates that the vehicle's electrical system is simplified to function at a fixed power level. To satisfy the vehicle's maximum speed (170 km/h) criterion, the maximum power of FC is set at 64.16 kW, with a backup power coefficient of 1.2 employed. This yields an approximate maximum power of 80 kW for the fuel cell, validating the previous theoretical calculations. Furthermore, to uphold the stability of the FC system, the minimum power is established based on the power consumption during cruising at 60 km/h, with a designated backup power considered, resulting in a final value of 10 kW. These power data are essential for researching the following power control strategy.

#### 2.4 PFC-optimized EMS for FCHEV

The primary goal of PFC strategy is ensuring Li-ion battery SOC remains within the optimal range, thereby achieving higher charge efficiency (D. Li *et al.*, 2020). It effectively minimizes electricity consumption by constraining the PEMFC's output power within a defined range and dynamically adjusting it to

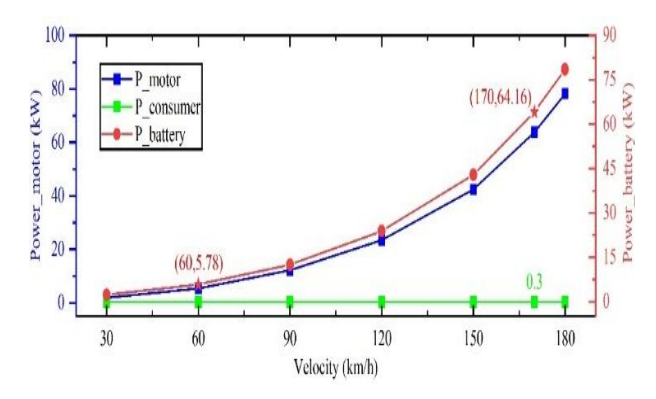


Fig. 5 Electrical power of battery, motor, and consumer of vehicle at various velocities

match the power demand (Ahmadi *et al.*, 2015). In this paper, to enhance the durability of the FC and avoid frequent toggling within the threshold, the FC start–stop process is optimized. The decision to turn the FC on or off relies not only on the battery SOC but also on the FC current working status. If the current SOC falls within the specified range, and the last status of the FC is in a working mode, then the FC generates power; if the FC is in an off mode, then the FC is turned off. This approach also guarantees long-term optimal operation of the Li-ion battery.

An ideal range for the SOC is established by the researchers. If the SOC falls below the anticipated level, the PEMFC needs to supply all the energy needs of the vehicle and to recharge the battery. If the SOC is within the set range, the PEMFC and battery work together, with the latter acting as a supplementary. If the SOC exceeds the designated range, the battery will provide the necessary power for the vehicle (Lü *et al.*, 2018). The PFC-optimized strategy segregates the motor into driving and braking modes. Whenever the vehicle speed exceeds 0.1, the braking pressure is above 0, and the SOC is below 0.9, the motor shifts into braking pattern. In this state, the battery serves to store the electric energy recuperated during braking, while the DC/DC converter remains inactive, not engaging in energy conversion. In the PFC-optimized strategy,

the operational states of the FC are grouped into the "working" mode, "wakeup" mode and "off "mode.

## 2.4.1 Control strategy in "wakeup" mode for FC system

The "wakeup" mode is happened when the vehicle initially starts. It is the precursor to "working" mode and requires a delay to warm up. During this time, the vehicle operates exclusively on battery power, and the battery power can be represented as

$$P_{battery} = P_{total} \tag{18}$$

where  $P_{total}$  is the demand power of the entire vehicle, which is the total of the FC air compressor power, resistance power, and the motor power.

#### 2.4.2 Control strategy in "working" mode for FC system

## 1. If the SOC falls below the minimum value, $soc < soc_{min}$

The power battery will be recharged by FC with minimized power output. The FC is responsible for delivering the total power required by the entire vehicle. Under these circumstances, the power allocation adheres to the subsequent equation.

$$P_{fc} = P_{fc\_max} \tag{19}$$

$$P_{battery} = P_{fc\ max} - P_{total} \tag{20}$$

where  $P_{fc\_max}$  is the FC maximum output power.

2. If the SOC is within the set range,  $soc_{min} < soc < soc_{max} \& FC_{last\ status} = 1$ 

When the SOC reaches its ideal value and the last status of the FC is in a working mode, the FC should primarily operate within its high-efficiency range to satisfy the power requirements of the overall vehicle. The FC power is conforming to Eq. (21).

$$P_{fc\_min} \le P_{fc} \le P_{fc\_max} \tag{21}$$

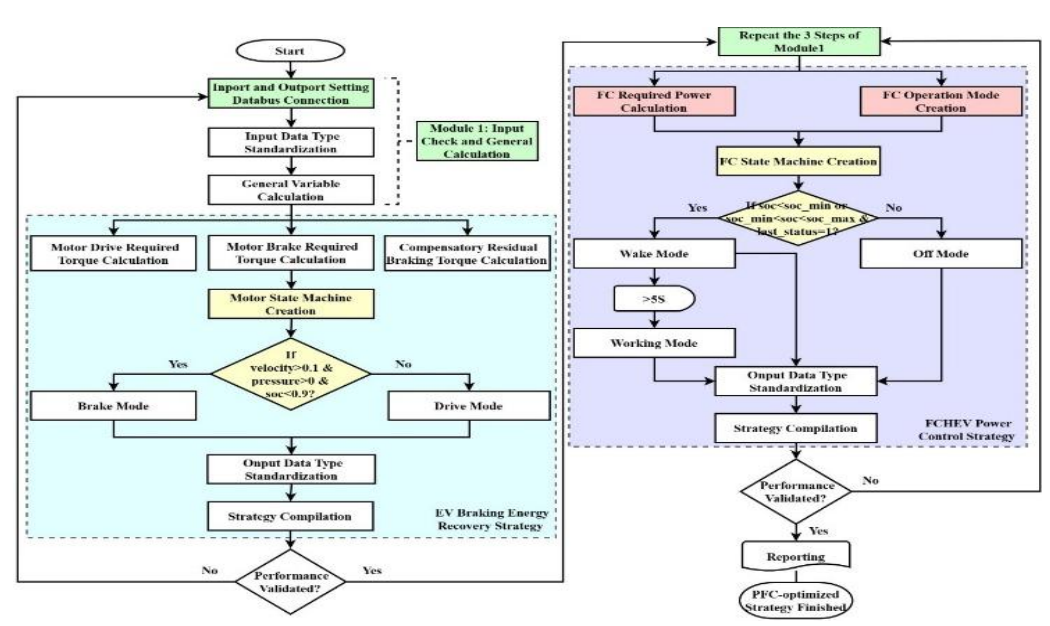


Fig. 6 PFC-optimized strategy modelling steps

where  $P_{fc\_min}$  is the FC minimum output power. If there is a need for extra power, the battery can provide additional peak power, and any surplus energy can be recovered by the battery. Eq. (22) can be used to calculate the battery output power.

$$P_{battery} = P_{total} - P_{fc} \tag{22}$$

## 2.4.3 Control strategy in "off" mode for FC system

When the SOC exceeds the maximum threshold,  $soc > soc_{max}$ , the battery fulfills the power demands of the whole vehicle, initiating its discharge until the SOC approaches the desired level. This encourages the efficient utilization of battery charge and ensures that the SOC stays within a specified threshold.

#### 2.5 EMS Modelling and Simulation

The PFC-optimized strategy is established in MATLAB/Simulink, consists of three modules, which are module 1: input check and general calculation, module 2: mode design and control volume calculation and module 3: state machine design and signal processing. The detailed modelling step is illustrated in Figure 6.

The first step of this strategy is operated in AVL CRUISE. "Inport" refers to the transfer of data from CRUISE to Simulink, while "Outport" refers to the transfer of data from Simulink to CRUISE. In the general variable calculation, Eq. (23) defines the instantaneous braking torque as below:

$$M_B = 2 \cdot p_B \cdot A_B \cdot \eta_B \cdot \mu_B \cdot r_B \cdot c_B \tag{23}$$

where  $M_B$ ,  $p_B$ ,  $A_B$ ,  $\eta_B$ ,  $\mu_B$ ,  $r_B$  and  $c_B$  are brake torque, brake pressure, brake piston surface, efficiency, friction coefficient, effective friction radius and specific brake factor (Disc brake,  $c_B = 1$ ), respectively. Therefore, Figure 8 shows the calculation of the brake factor for the rear and front axles, where the parameters are sourced from CRUISE's "Disc Brake" modules.

The entire construction process is based on two key logics, namely the "EV Braking Energy Recovery Strategy" and the "FCHEV Power Control Strategy", with the former serving as the foundation for the latter. The steps represented in the yellow box in the figure denote the core of module 3, which involves the establishment of two state machines to switch between the motor drive and brake modes, as well as among the three operational modes of the fuel cell. The operations depicted in the red box belong to module 2, as seen in Figure 7, which is the crucial aspect in EMS calculations and specifies the additional power required from the FC system.

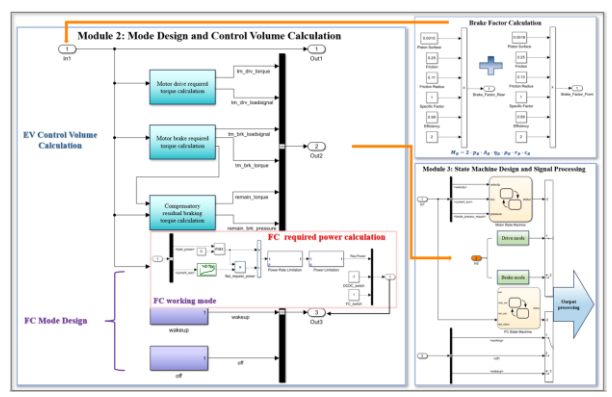


Fig. 7 Schematic of PFC-optimized strategy

#### 3. Results and discussion

## 3.1 Selection of simulation conditions and dynamics validation

Different driving cycles necessitate varying motor output powers. This study selects the CLTC-P as a representative driving cycle to comprehensively evaluate vehicle performance. The CLTC-P is defined in GB/T38146.1-2019 "China automotive test cycle- Part 1: Light-duty vehicles" and forms part of the China automotive test cycle (CATC) developed by the China Automotive Technology & Research Center (CATARC) in 2019 (Duan et al., 2021). According to the Chinese government's mandate, all domestically sold new energy vehicles must conform to the CLTC standard by 2025, replacing the previous New European Driving Cycle (NEDC) standard. Notably, the CLTC lacks a definition for extra-high-speed sections, aligning with China's expressway speed limit of 120km/h. The CLTC-P exhibits a low average velocity with frequent accelerations and decelerations, mirroring the typical daily travel conditions of Chinese consumers. Consequently, the cruising range under CLTC conditions surpasses that of the NEDC. Given the potential drawbacks of a significantly higher cruising range for consumers, this study also includes NEDC and the Word Light Vehicle Test Cycle (WLTC) for comparison. Figure 8 illustrates that the PFC-optimized strategy proposed in this paper effectively achieves speed control under various driving cycle conditions, meeting the performance criteria for the entire vehicle. Table 3 displays the primary parameters.

In the created simulation task folder, in accordance with the national standard, the performance evaluation of FCHEV encompasses assessments of acceleration, maximum vehicle speed, and uphill ability test at different vehicle velocities. Figure 9 presents the simulation outcomes for acceleration performance, indicating that the vehicle achieves speeds exceeding 50 km/h from a standstill (0 km/h) in 4.18 s, meeting the design criterion of  $\leqslant 5$  s. The findings regarding the vehicle

**Table 3**Characteristics of the three driving conditions

Characteristics of the three driving conditions					
Characteristics	NEDC	CLTC-P	WLTC		
Total time (s)	1180	1800	1800		
Driving distance (km)	10.927	14.486	23.276		
Maximum speed (km/h)	120.44	114.07	131.35		
Average speed (including stops) (km/h)	33.47	29.04	46.68		

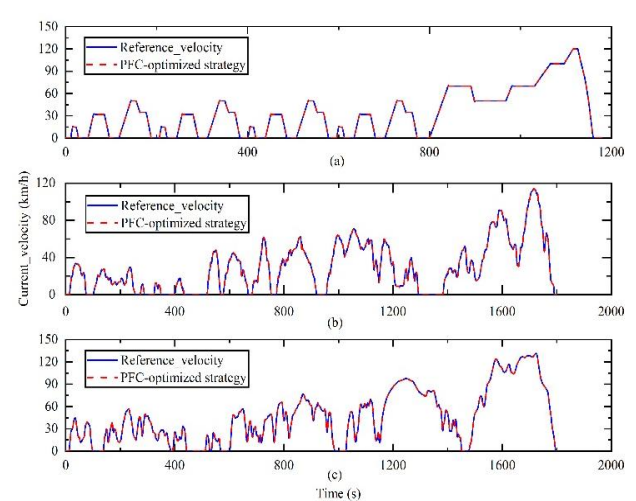


**Fig. 8** Speed following with PFC-optimized strategy in different driving cycles: (a) NEDC, (b) CLTC-P, and (c) WLTC

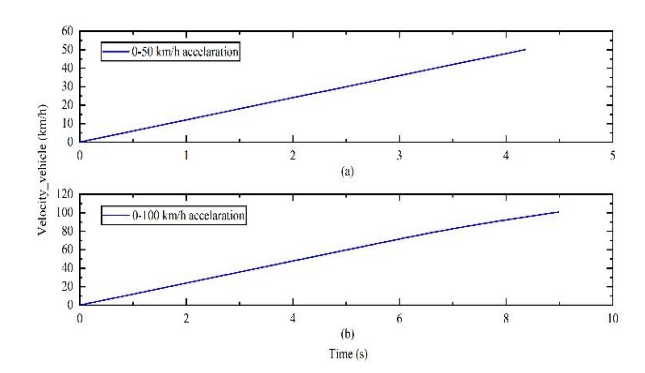


Fig. 9 Acceleration performance: (a) 0-50 km/h acceleration. (b) 0-100 km/h acceleration

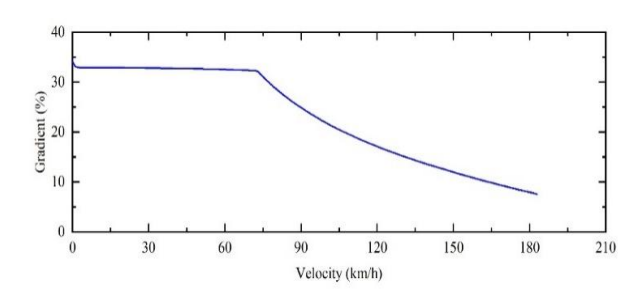


Fig. 10 Maximum gradient curve of vehicle with speed

acceleration capabilities from 0 to 100 km/h indicate that the vehicle attains speeds surpassing 100 km/h from a standstill (0 km/h) in 8.9 s, adhering to the design requirement of  $\leq 10$  s. Moreover, the "Constant Drive max velocity" result report reveals that the maximum vehicle speed reaches 182 km/h.

The climbing capability on maximum slope in hybrid mode of an electric vehicle refers to the maximum angle between the horizontal plane and the inclined surface at which the vehicle can travel at a certain speed (Deng et al., 2019). In terms of the powertrain system, ascending a slope necessitates the generation of sufficient forces to prevent tire slippage. Insufficient energy may hinder the vehicle's ability to ascend, highlighting the significance of the maximum gradient in reflecting the vehicle's power performance and its capacity to endure maximum pressure. The simulation results in Figure 10 illustrate the maximum gradient under different vehicle speeds for the fuel cell power system. The FCHEV achieves a maximum gradient of 34.23%. The maximum gradients at velocities of 30 km/h and 60 km/h are 32.86% and 32.54%, separately. These

Table 4 Test result of the ECHEV

Type of index	Description	Simulation result	Design goal
Maximum speed	Maximum speed (km/h)	182	≥170
Acceleration	0-50 km/h (s)	4.18	≤5
ability	0-100 km/h (s)	8.90	≤10
Climbing ability	Maximum grade	34.23	≥30
	Maximum grade @30km/h (%)	32.86	≥12
	Maximum grade @60km/h (%)	32.54	≥4
Cruising range	@60km/h (km)	70.332	≥65

performance simulation findings, as summarized in Table 4, all meet the vehicle's performance indexes.

#### 3.2 Comparison and analysis of economic property

To verify the efficacy and viability of the suggested EMSs, the "MATLAB\_DLL" control strategy module in AVL CRUISE integrated the PFC strategy and the PFC-optimized control strategy separately. This comprehensive integration supported the creation of the entire vehicle simulation model, allowing for the evaluation and comparison of the simulation outcomes from the EMSs (Zou et al., 2023).

Figure 11 presents a comparison of the SOC performance across the two suggested strategies under the NEDC, CLTC-P, and WLTC driving conditions. It is evident that all SOC trajectories remain within acceptable limits (from 0.5 to 0.7). This range is in line with the vehicle's operational requirements. preventing instances of overcharging or over discharging of the battery. Such management practices are beneficial for extending the overall lifespan of the battery (D. Li et al., 2020). Additionally, a comparative analysis of the two strategies reveals that the PFC strategy exhibits a relatively larger SOC fluctuation range, with the absolute difference between the final and initial SOC (|\Delta SOC|) spanning from 1.8% to 9.4%. In contrast, the implementation of the PFC-optimized strategy, which incorporates the final state of the FC condition, yields a stable profile SOC  $(1.39\% < |\Delta SOC| < 3.87\%),$ characterized by shallower charge-discharge cycles. Notably, under the CLTC-P operation, this strategy demonstrates exceptional SOC retention, with a variance of only 1.39%, marking a reduction of approximately 3.07% compared to the conventional PFC approach. The most significant enhancement is observed under the NEDC operation, where the PFCoptimized EMS mitigates SOC fluctuations, resulting in a 6.52% lower remaining SOC than the PFC strategy. Overall, these

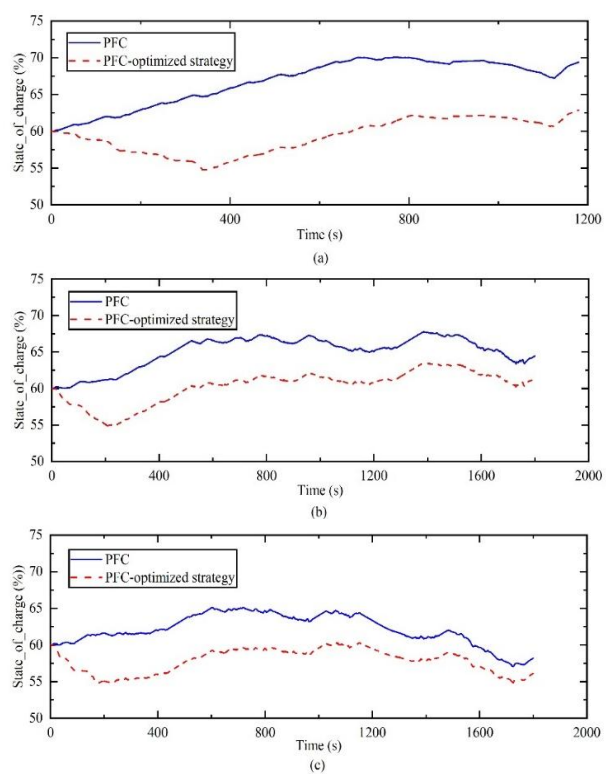
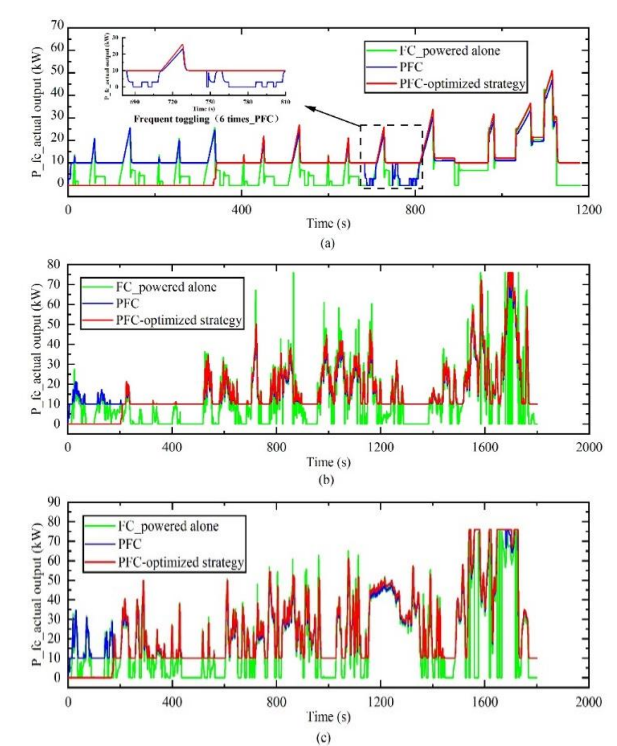


Fig. 11 SOC in different driving cycles: (a) NEDC, (b) CLTC-P, and (c) WLTC



**Fig. 12** Fuel cell actual output power in different driving cycles: (a) NEDC, (b) CLTC-P, and (c) WLTC

improvements effectively contribute to enhancing battery life and reducing vehicle maintenance costs, addressing a critical concern among users.

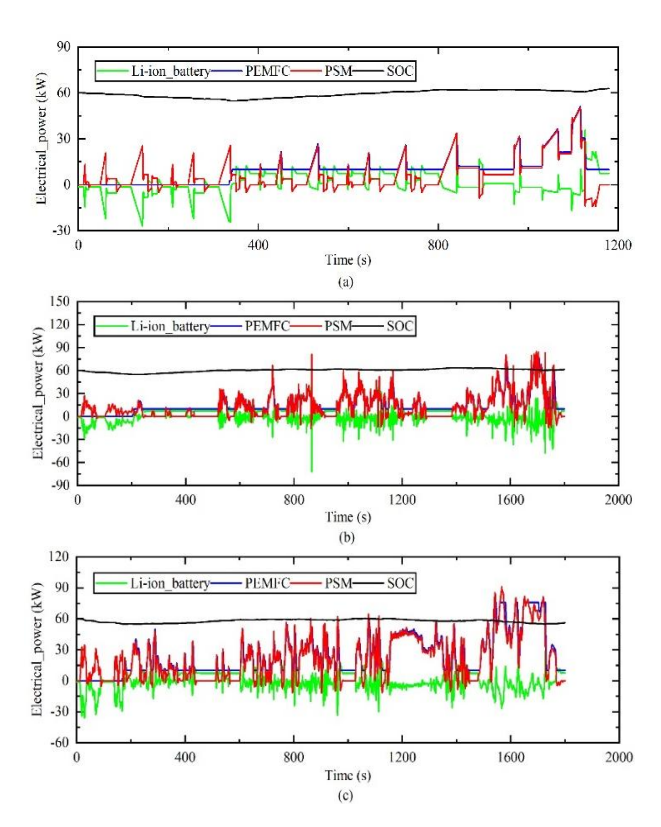
The simulation outcomes demonstrate the actual output power of the PEMFC under three different scenarios: the PFCoptimized strategy, the PFC, and the FC standalone power supply. Figure 12 depicted that, under the PFC-optimized strategy, the FC's output power fluctuates within the range of 10 kW to 80 kW, meeting the prescribed boundaries for the power output of the FC. Besides, the FC can operate within an efficiency range exceeding 45%. Generally, the variation in the FC output power is narrower when using the PFC-optimized strategy compared to other two EMSs. Compared to operating the FC as the sole power source, the PFC EMS effectively reduces frequent FC toggling by 94% across all three driving conditions. Notably, under the NEDC operation, the PFCoptimized strategy eliminates the fuel cell's recurrent start-stop cycles, reducing them from 6 to 0. This indicates that the utilization of the PFC-optimized strategy results in a more stable and consistent FC output power, enabling uninterrupted and continuous operation, thereby effectively enhancing the durability of the FC.

Figure 13 depicts the power distribution and SOC under the PFC-optimized EMS across three operating conditions. The initial SOC is 0.6, enabling sufficient power provision for motor startup. With the incorporation of FC state control, the fuel cell initially operates in the "wakeup" mode when the vehicle's power demand is low. This not only helps maintain battery SOC but also extends the fuel cell's lifespan. The graphical analysis reveals that the peak transient power during acceleration and deceleration reaches approximately 55 kW and 15 kW under NEDC, 85 kW and 15 kW under CLTC-P, and 90 kW and 15 kW under WLTC, respectively. In practical scenarios, such as during CLTC-P operating conditions, spanning from 0 to 203 s, the battery powers the entire vehicle independently. Afterward, the FC assumes the role of recharging the battery. During

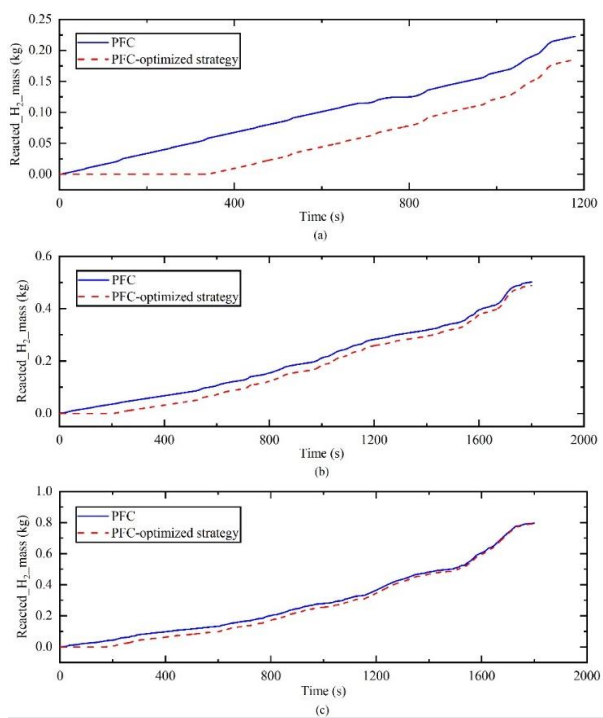
periods of frequent acceleration and deceleration, where substantial power demands are evident, both the battery and FC collaborate to drive the vehicle. Post 1696 s, peak power demand reaches 85.07 kW, with both the battery and fuel cell supplying power simultaneously, thereby resulting in a moderated descent across all curves. Following the braking phases after 1730 s, regenerative braking facilitates a universal rebound in both SOC and the electrical power of Li-ion battery across all curves. The actual power distribution in the other two driving cycles follows the same pattern as in the CLTC-P cycle, adhering to the design principles of the PFC-optimized EMS. Consequently, this strategy extends the operational life expectancy of the battery while obviating the necessity for an external battery charger.

Figure 14 provides a comparative analysis of hydrogen consumption between the two strategies under three driving conditions. The hydrogen consumption declines from 0.223 kg to 0.185 kg under NEDC, from 0.502 kg to 0.488 kg under CLTC-P, and from 0.797 kg to 0.790 kg under WLTC. Compared to the conventional PFC EMS, the PFC-optimized strategy achieves reductions of approximately 17.04%, 2.79%, and 0.88% under NEDC, CLTC-P, and WLTC, respectively. These findings clearly indicate that the optimized strategy significantly improves fuel economy across all three driving conditions, with the most pronounced enhancement observed in the NEDC cycle.

Furthermore, Table 5 reinforces that the PFC-optimized strategy achieves the lowest hydrogen consumption per 100 km, decreasing from 2.038 kg/100 km to 1.696 kg/100 km under NEDC, from 3.463 kg/100 km to 3.369 kg/100 km under CLTC-P, and from 3.432 kg/100 km to 3.407 kg/100 km under WLTC. This translates to fuel consumption improvements



**Fig. 13** Electrical power and SOC of FCHEV under PFC-optimized strategy in different driving cycles: (a) NEDC, (b) CLTC-P, and (c) WLTC



**Fig. 14** Comparisons of hydrogen consumption: (a) NEDC, (b) CLTC-P, and (c) WLTC

**Table 5** Hydrogen consumption per 100 km in different conditions

Driving Condition	PFC	PFC-	Rate of change of
	(kg/100	optimized	hydrogen
	km)	(kg/100 km)	consumption (%)
NEDC	2.038	1.696	-16.78
CLTC-P	3.463	3.369	-2.71
WLTC	3.432	3.407	-0.7

ranging from 0.7% to 16.78%. Overall, these results highlight the superior fuel economy of the PFC-optimized strategy.

## 4. Conclusion

This study introduces the design of the powertrain for an FCHEV along with the calculation of key component parameters. It elaborates on the precise modeling of the vehicle module using the simulation software AVL CRUISE, which is secondly developed. Also, the CLTC-P driving cycle is introduced. Recognizing the pivotal role of EMS in vehicle performance, the PFC-optimized strategy is developed in MATLAB/Simulink for the FCHEV under study. This strategy utilizes PFC to optimize the FC output power to the optimal operating point derived from the battery SOC, while considering the status of FC operating mode to prevent frequent toggling within the threshold.

Both the PFC and the proposed PFC-optimized strategy demonstrate compliance with dynamic performance requirements and achieve speed tracking for the NEDC, CLTC-P, and WLTC driving cycles. Simulation findings of FC actual output power indicate that the addition of the battery enhances overall vehicle power, particularly during scenarios requiring high power such as startup and acceleration, thereby alleviating peak power pressure on the FC. Additionally, the SOC and life of battery, along with fuel economy and fuel cell durability, are key results obtained through the PFC-optimized strategy.

Implementation of this strategy results in smoother SOC profiles compared to the PFC strategy. The Li-ion battery can enable sufficient power provision for motor startup and the fuel cell is engaged to initiate battery charging after a short time. Thus, the battery's operational lifespan is prolonged, leading to reduced vehicle maintenance costs. Moreover, across all three driving cycles, the PFC-optimized strategy exhibits higher efficiency and reduced hydrogen consumption compared to the PFC strategy, thereby demonstrating superior economy and operational durability. These research findings and the proposed strategy can serve as valuable references for future studies.

## Acknowledgments

The authors would like to thank Universiti Putra Malaysia (UPM) and the Chongqing Electric Power College (CQEPC), for their continuous support in the research work.

**Author Contributions**: Leipengyun Deng: Conceptualization, methodology, formal analysis, writing—original draft. Mohd Amran Mohd Radzi: supervision, project administration, validation, writing—review & editing. Suhaidi Shafie: validation, writing—review & editing. Mohd Khair Hassan: validation, writing—review & editing. All authors have read and agreed to the published version of the manuscript.

**Funding:** The author(s) received no financial support for the research, authorship, and/or publication of this article.

Conflicts of Interest: The authors declare no conflict of interest.

## References

Ahmadi, S., Bathaee, S. M. T., & Hosseinpour, A. H. (2018). Improving fuel economy and performance of a fuel-cell hybrid electric vehicle (fuel-cell, battery, and ultra-capacitor) using optimized energy management strategy. *Energy Conversion and Management*, 160, 74-84. https://doi.org/10.1016/j.enconman.2018.01.020

Ahmadi, S., & Bathaee, S. M. T. (2015). Multi-objective genetic optimization of the fuel cell hybrid vehicle supervisory system: Fuzzy logic and operating mode control strategies. *International Journal of Hydrogen Energy*, 40(36), 12512-12521. https://doi.org/10.1016/j.ijhydene.2015.06.160

Bizon, N., Bizon, N., & Thounthong, P. (2018). Fuel economy using the global optimization of the Fuel Cell Hybrid Power Systems. *Energy Conversion and Management*, 173, 665-678. https://doi.org/10.1016/j.enconman.2018.08.015

Deng, H., Zhang, Y., Fang, R., & Pei, Z. (2019). Study on Fuel Cell Vehicle Power System Selection and Simulation. *In 2019 IEEE 4th Advanced Information Technology, Electronic and Automation Control Conference (IAEAC)* (pp. 2382-2385). IEEE. https://doi.org/10.1109/IAEAC47372.2019.8997909

Du, C., Huang, S., Jiang, Y., Wu, D., & Li, Y. (2022). Optimization of energy management strategy for fuel cell hybrid electric vehicles based on dynamic programming. *Energies*, 15(12), 4325. https://doi.org/10.3390/en15124325

Duan, Z., Mei, N., Feng, L., Yu, S., Jiang, Z., Chen, D., ... & Hong, J. (2021). Research on hydrogen consumption and driving range of hydrogen fuel cell vehicle under the CLTC-P condition. World Electric Vehicle Journal, 13(1), 9. https://doi.org/10.3390/wevj13010009

Geng, C., Jin, X., & Zhang, X. (2019). Simulation research on a novel control strategy for fuel cell extended-range vehicles. *International Journal of Hydrogen Energy*, 44(1), 408-420. https://doi.org/10.1016/j.ijhydene.2018.04.038

Gharibeh, H. F., Yazdankhah, A. S., & Azizian, M. R. (2020). Energy management of fuel cell electric vehicles based on working condition identification of energy storage systems, vehicle

- driving performance, and dynamic power factor. *Journal of Energy Storage*, 31, 101760. https://doi.org/10.1016/j.est.2020.101760
- Hosseini, S. E., & Butler, B. (2020). An overview of development and challenges in hydrogen powered vehicles. *International journal of green energy*, 17(1), 13-37. https://doi.org/10.1080/15435075.2019.1685999
- Hu, J., Wang, Z., Du, H., & Zou, L. (2022). Hierarchical energy management strategy for fuel cell/ultracapacitor/battery hybrid vehicle with life balance control. *Energy Conversion and Management*, 272, 116383. https://doi.org/10.1016/j.enconman.2022.116383
- Hu, X., Liu, S., Song, K., Gao, Y., & Zhang, T. (2021). Novel fuzzy control energy management strategy for fuel cell hybrid electric vehicles considering state of health. *Energies*, 14(20), 6481. https://doi.org/10.3390/en14206481
- İnci, M., Büyük, M., Demir, M. H., & İlbey, G. (2021). A review and research on fuel cell electric vehicles: Topologies, power electronic converters, energy management methods, technical challenges, marketing and future aspects. In *Renewable and Sustainable Energy Reviews* (Vol. 137). https://doi.org/10.1016/j.rser.2020.110648
- Jia, X., & Zhao, M. (2023). A Hierarchical Energy Control Strategy for Hybrid Electric Vehicle with Fuel Cell/Battery/Ultracapacitor Combining Fuzzy Controller and Status Regulator. *Electronics*, 12(16), 3428. https://doi.org/10.3390/electronics12163428
- Jung, J., Kim, D., Yang, L., & Kim, N. (2024). Optimal Energy
  Management Strategy for Repeat Path Operating Fuel Cell
  Hybrid Tram. *Energies*, 17(7), 1560.
  https://doi.org/10.3390/en17071560
- Kim, Y., Han, J., & Yu, S. (2023). Establishment of energy management strategy of 50 kW PEMFC hybrid system. *Energy Reports*, 9, 2745-2756. https://doi.org/10.1016/j.egyr.2023.01.096
- Kulikovsky, A. A. (2013). A Physically–Based Analytical Polarization Curve of a PEM Fuel Cell. Journal of The Electrochemical Society, 161(3), F263–F270. https://doi.org/10.1149/2.028403JES/META
- Li, D., Xu, B., Tian, J., & Ma, Z. (2020). Energy management strategy for fuel cell and battery hybrid vehicle based on fuzzy logic. *Processes*, 8(8). https://doi.org/10.3390/PR8080882
- Li, G., Chen, J., Zheng, X., Xiao, C., & Zhou, S. (2020). Research on Energy Management Strategy of Hydrogen Fuel Cell Vehicles. Proceedings - 2020 Chinese Automation Congress, CAC 2020, 7604–7607. https://doi.org/10.1109/CAC51589.2020.9326669
- Li, W., Xu, H., Liu, X., Wang, Y., Zhu, Y., Lin, X., Wang, Z., & Zhang, Y. (2024). Regenerative braking control strategy for pure electric vehicles based on fuzzy neural network. *Ain Shams Engineering Journal*, 15(2). https://doi.org/10.1016/j.asej.2023.102430
- Li, Y., He, H., Peng, J., & Wang, H. (2019). Deep reinforcement learning-based energy management for a series hybrid electric vehicle enabled by history cumulative trip information. *IEEE Transactions on Vehicular Technology*, 68(8), 7416–7430. https://doi.org/10.1109/TVT.2019.2926472
- Lin, C., Luo, W., Lan, H., & Hu, C. (2022). Research on multi-objective compound energy management strategy based on fuzzy control for FCHEV. *Energies*, 15(5), 1721. https://doi.org/10.3390/en15051721
- Liu, C., Lin, H., Shi, C., & Hu, M. (2024). Development status and outlook of hydrogen powered fuel cell vehicle market in China. *Southern energy construction*, 11(2): 162-171. https://doi.org/10.16516/j.ceec.2024.2.03
- Lü, X., Qu, Y., Wang, Y., Qin, C., & Liu, G. (2018). A comprehensive review on hybrid power system for PEMFC-HEV: Issues and strategies. *Energy conversion and Management*, 171, 1273-1291. https://doi.org/10.1016/j.enconman.2018.06.065
- Lü, X., Wu, Y., Lian, J., Zhang, Y., Chen, C., Wang, P., & Meng, L. (2020). Energy management of hybrid electric vehicles: A review of energy optimization of fuel cell hybrid power system based on genetic algorithm. In *Energy Conversion and Management* (Vol. 205). https://doi.org/10.1016/j.enconman.2020.112474
- Luca, R., Whiteley, M., Neville, T., Shearing, P. R., & Brett, D. J. L. (2022). Comparative study of energy management systems for a hybrid fuel cell electric vehicle - A novel mutative fuzzy logic

- controller to prolong fuel cell lifetime. *International Journal of Hydrogen Energy*, 47(57), 24042–24058. https://doi.org/10.1016/j.ijhydene.2022.05.192
- Ou, K., Yuan, W. W., Choi, M., Yang, S., Jung, S., & Kim, Y. B. (2018).

  Optimized power management based on adaptive-PMP algorithm for a stationary PEM fuel cell/battery hybrid system.

  International journal of hydrogen energy, 43(32), 15433-15444. https://doi.org/10.1016/j.ijhydene.2018.06.072
- Peng, H., Chen, Z., Deng, K., Dirkes, S., Ünlübayir, C., Thul, A., ... & Hameyer, K. (2021). A comparison of various universally applicable power distribution strategies for fuel cell hybrid trains utilizing component modeling at different levels of detail: From simulation to test bench measurement. *ETransportation*, 9, 100120. https://doi.org/10.1016/j.etran.2021.100120
- Reddy, N. P., Pasdeloup, D., Zadeh, M. K., & Skjetne, R. (2019). An intelligent power and energy management system for fuel cell/battery hybrid electric vehicle using reinforcement learning. In 2019 IEEE transportation electrification conference and expo (ITEC) (pp. 1-6). IEEE. https://doi.org/10.1109/ITEC.2019.8790451
- Shen, Y., Cui, P., Wang, X., Han, X., & Wang, Y. X. (2020). Variable structure battery-based fuel cell hybrid power system and its incremental fuzzy logic energy management strategy. *International Journal of Hydrogen Energy*, 45(21), 12130-12142. https://doi.org/10.1016/j.ijhydene.2020.02.083
- Song, K., Li, F., Hu, X., He, L., Niu, W., Lu, S., & Zhang, T. (2018). Multimode energy management strategy for fuel cell electric vehicles based on driving pattern identification using learning vector quantization neural network algorithm. *Journal of Power Sources*, 389, 230-239. https://doi.org/10.1016/j.jpowsour.2018.04.024
- Teng, T., Zhang, X., Dong, H., & Xue, Q. (2020). A comprehensive review of energy management optimization strategies for fuel cell passenger vehicle. *International Journal of Hydrogen Energy*, 45(39), 20293–20303. https://doi.org/10.1016/j.ijhydene.2019.12.202
- Tian, X., Tao, F., Fu, Z., Zhu, L., Sun, H., & Song, S. (2024). Optimizing fuel economy of fuel cell hybrid electric vehicle based on energy management strategy with integrated rapid thermal regulation. *Engineering Applications of Artificial Intelligence*, 132, 107880. https://doi.org/10.1016/j.engappai.2024.107880
- Wang, Y., Zhang, Y., Zhang, C., Zhou, J., Hu, D., Yi, F., Fan, Z., & Zeng, T. (2023). Genetic algorithm-based fuzzy optimization of energy management strategy for fuel cell vehicles considering driving cycles recognition. *Energy*, 263. https://doi.org/10.1016/j.energy.2022.126112
- Xu, J., Zhang, C., Fan, R., Bao, H., Wang, Y., Huang, S., ... & Li, C. (2020). Modelling and control of vehicle integrated thermal management system of PEM fuel cell vehicle. *Energy*, 199, 117495. https://doi.org/10.1016/j.energy.2020.117495
- Yang, N., Han, L., Xiang, C., Liu, H., & Hou, X. (2021). Energy management for a hybrid electric vehicle based on blended reinforcement learning with backward focusing and prioritized sweeping. *IEEE Transactions on Vehicular Technology*, 70(4), 3136-3148. https://doi.org/10.1109/TVT.2021.3064407
- Zhang, Q., & Li, G. (2019). A Game Theory Energy Management Strategy for a Fuel Cell/Battery Hybrid Energy Storage System. Mathematical Problems in Engineering, 2019. https://doi.org/10.1155/2019/7860214
- Zhang, Y., Zhang, C., Huang, Z., Xu, L., Liu, Z., & Liu, M. (2019). Real-Time Energy Management Strategy for Fuel Cell Range Extender Vehicles Based on Nonlinear Control. *IEEE Transactions on Transportation Electrification*, 5(4), 1294–1305. https://doi.org/10.1109/TTE.2019.2958038
- Zhang, Y., Lü, X., Wang, M., & Gu, D. (2021). Output Power Follow-up Research of Fuel Cell Hybrid Power System. *Journal of Shanghai University of Electric Power*, 37(2): 109-114. https://doi.org/10.3969/j.issn.2096-8299.2021.02.002
- Zhao, Z., Wang, T., Li, M., Wang, H., & Wang, Y. (2021). Optimization of fuzzy control energy management strategy for fuel cell vehicle power system using a multi-islandgenetic algorithm. *Energy Science and Engineering*, 9(4), 548–564. https://doi.org/10.1002/ese3.835

Zou, K., Luo, W., & Lu, Z. (2023). Real-Time Energy Management Strategy of Hydrogen Fuel Cell Hybrid Electric Vehicles Based on Power Following Strategy–Fuzzy Logic Control Strategy Hybrid Control. World Electric Vehicle Journal, 14(11), 315. https://doi.org/10.3390/wevj14110315



© 2025. The Author(s). This article is an open access article distributed under the terms and conditions of the Creative Commons Attribution-ShareAlike 4.0 (CC BY-SA) International License (http://creativecommons.org/licenses/by-sa/4.0/)